

Solvent-polarizability dependence of the relative $2^1A_g(S_1)$ - and $1^1B_u(S_2)$ -fluorescence intensities of 1,14-diphenyl-1,3,5,7,9,11,13-tetradecaheptaene

Takao Itoh^{a)}

Chemistry Department, Miyazaki Medical College, Miyazaki 889-1692, Japan

(Received 31 March 2003; accepted 21 May 2003)

Emission, excitation, and absorption spectra of diphenyltetradecaheptaene (DP7) have been measured in solvents with different polarizabilities, together with the Raman spectrum at room temperature. DP7 exhibits dual fluorescence from the $2^1A_g(S_1)$ and $1^1B_u(S_2)$ states in room temperature solution. It is shown that the $2^1A_g/1^1B_u$ fluorescence intensity-ratio varies significantly depending on the solvent polarizability. This observation was interpreted on the basis of the coupling strength between the $2^1A_g/1^1B_u$ states which is determined mainly by the $2^1A_g-1^1B_u$ energy separation. Fitting of the spectra with sum of Gaussians reveals a significant difference in Franck–Condon envelop between the 2^1A_g and 1^1B_u fluorescence spectra, which is originating from the large difference in the C–C and C=C stretching mode displacements between the 2^1A_g and 1^1B_u states. © 2003 American Institute of Physics. [DOI: 10.1063/1.1591172]

I. INTRODUCTION

Polyene chromophores play important roles in photobiology such as vision and energy production. A detailed understanding of the electronic structure of conjugated linear polyenes is fundamental to understanding complicated processes in biological systems as well as the charge transport in conducting polymers. Among a number of polyene molecules, diphenylpolyenes have been the subject of a number of spectroscopic investigations, not only because these polyenes are strongly fluorescent and commercially available, but also because such studies advance our understanding of polyene electronic structure and the connection between that structure and spectroscopic properties.^{1–5}

Indeed, the first part of the above sentence applies for diphenylpolyenes with the polyene double bond number (n) from one to four. However, the situation is somewhat different for diphenylpolyenes with n over five. These longer diphenylpolyenes are not only commercially unavailable but also weakly fluorescent, although the details of the emission properties of diphenylpolyenes with $n=5$ and 6 have already been reported.^{6,7} The emission spectrum of diphenylpolyene with $n=7$, diphenyltetradecaheptaene (DP7, Fig. 1), has not been reported until recently, presumably because of the weakness of the emission and the low solubility of the sample as well as the red emission region.⁸ In the emission spectrum of DP7 reported recently, both of the $2^1A_g(S_1)$ and $1^1B_u(S_2)$ fluorescence are presented.⁸ Thus, it must be of interest to investigate the spectroscopic properties of DP7 more in detail, since we can obtain the information on the nature and the interaction of the two excited states directly through the measurement of the dual emission which is a kind of unusual phenomenon.

In the present study, emission, excitation, and absorption

spectra of DP7 have been measured in solvents with different polarizabilities at room temperature, together with the Raman spectrum. It was shown that the $2^1A_g/1^1B_u$ fluorescence-intensity ratio depends significantly on the solvent polarizability. This observation was interpreted on the basis of the coupling strength between the 2^1A_g and 1^1B_u states which depends mainly on the $2^1A_g-1^1B_u$ energy separation. Further, all the measured spectra were reproduced reasonably by superposition of Gaussians. The calculated spectra of DP7 revealed a significant difference in Franck–Condon envelop between the 2^1A_g and 1^1B_u fluorescence spectra. The results of the Franck–Condon analyses of the emission and absorption spectra showed that there is a large difference in the C=C and C–C, stretching mode displacements between the 2^1A_g and 1^1B_u states, which seems to be an excited-state character common to all the fluorescent polyenes.

II. EXPERIMENT

Diphenyltetradecaheptaene (DP7) was synthesized according to the procedure reported by Spangler *et al.*⁹ and recrystallized repeatedly from a mixture of dimethylformamide and toluene. Diiodomethane (methyleneiodide) obtained from Aldrich, USA and 1-bromonaphthalene obtained from Wako Pure Chemicals, Japan were used without further purification, after we confirmed that these solvents contained no impurities that emitted under the conditions of the present experiment. Other solvents used are all of spectroscopic grade.

Absorption spectra were measured with a Shimadzu UV-2550 spectrophotometer, with which the optical densities as low as 3×10^{-3} can be measured with a reasonable S/N ratio. Emission and excitation spectra were measured with a Spex Fluorolog-3 (Model 21-SS) spectrophotometer, equipped with a double-grating excitation monochromator, a

^{a)}Electronic mail: tioth@fc.miyazaki-med.ac.jp

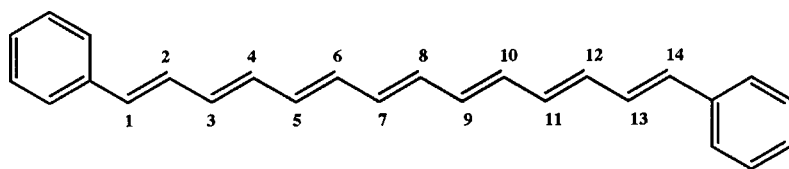


FIG. 1. Molecular structure of diphenyltetradecaheptaene (DP7).

1, 14-Diphenyl-1, 3, 5, 7, 9, 11, 13-tetradecaheptaene (DP7)

high-pressure 450-W xenon lamp as an excitation-light source, and a photomultiplier tube (Hamamatsu R928-P) in an electric-cooled housing operated in photon-counting mode. A Melles Griot He-Ne green laser (5435 Å, 1.5 mW) was used as the excitation light source for measurement of Raman spectrum. The laser beam passing through the sample cell was reflected by a mirror behind the cell holder to intensify the laser light. Raman light from the sample scattered perpendicular to the laser beam was dispersed and detected with a system of a Spex Fluorolog-3 spectrophotometer. For most of the emission measurements square 10-mm path length quartz cells were used. A cylindrical 100-mm path length quartz cell was also used for measurements of weak absorption. Raman and Rayleigh scattering light from the solvents were subtracted from the measured emission spectra as well as from the measured Raman spectrum of DP7. Special care was taken so as to measure the emission spectra of the samples, and Raman and Rayleigh scattering spectra of the solvents exactly in the same condition. Sample solution

in a cell was changed using a filtered injection without replacing the cell in a cell holder. It was confirmed also that undissolved microcrystals of DP7 were not contained in the sample cell.

Emission spectra were corrected for the spectral sensitivity of the detection system by comparing the measured spectrum with the real spectrum using *N,N*-dimethylnitroaniline in a hexane-benzene mixture as a standard which shows the emission ranging from 12 000 to 22 000 cm^{-1} .¹⁰ Excitation spectra were corrected for the spectral intensity distribution of the exciting light with an aqueous solution of rhodamine B as a quantum counter. Fluorescence quantum yields were determined by comparing the corrected fluorescence spectra of the DP7 solutions with that of diphenylhexatriene solution which is known to have a fluorescence quantum yield of 0.8.⁷ Digital data were analyzed with a Macintosh Quadra 650 computer loaded with a super PC memory and with a Power Macintosh G4 computer.

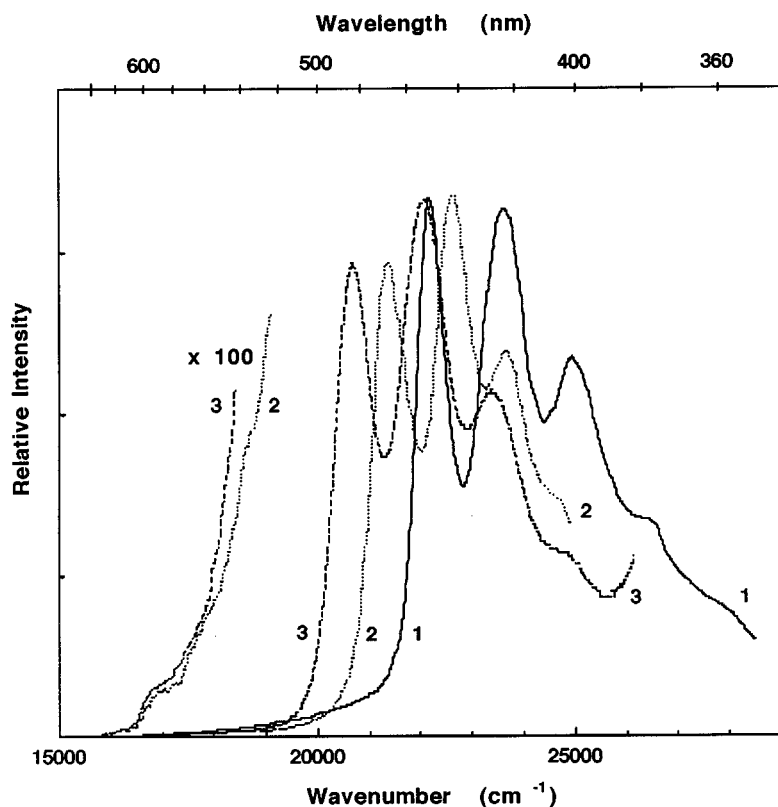


FIG. 2. Absorption spectra of DP7 in hexane (1), *N,N*-dimethylformamide (2) and CS_2 (3) at 18 °C. All the spectra are normalized to a common magnitude.

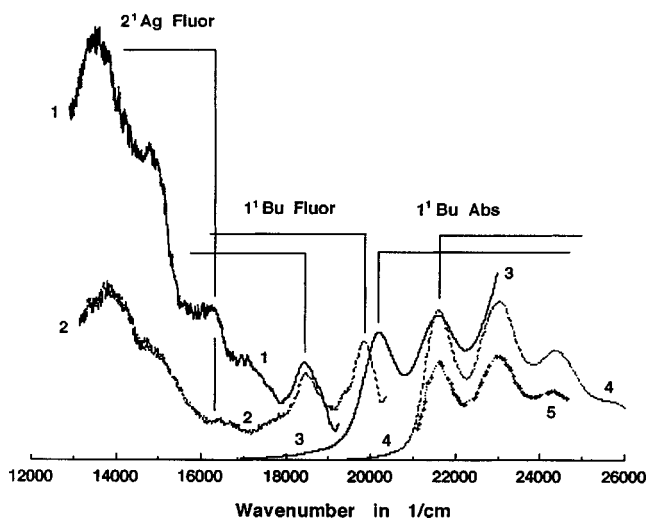


FIG. 3. Corrected emission (1 and 2), absorption (3 and 4) and corrected excitation spectra (5) of DP7 in diiodomethane (methyleneiodide) (1 and 3) and in carbon tetrachloride (2, 4, and 5) at 18 °C.

III. RESULTS AND DISCUSSION

Figure 2 shows the absorption spectra of DP7 in solvents with different polarizabilities at room temperature. It is clearly seen that the strong $1^1A_g(S_0) \rightarrow 1^1B_u(S_2)$ absorption band shifts to the red with increasing the solvent polarizability. Closer inspection of the spectra reveals that there is also a very weak absorption band observed at near 16670 cm^{-1} (600 nm), the relative intensity of which is weaker than that of the first $1^1A_g \rightarrow 1^1B_u$ absorption band by a factor of approximately 3×10^{-4} . This weak band does not show a significant shift with changing the solvent polarizability. In light of the location of the $2^1A_g(S_1)$ fluorescence spectrum (*vide infra*) and the weakness of the absorption, the observed weak band can be most probably attributed to the transition to the one-photon forbidden and two-photon allowed 2^1A_g state.

Emission, absorption, and excitation spectra of DP7 in two solvents with different polarizabilities are presented in Fig. 3. The measured emission spectrum can be separated into the blue spectrum starting from about 20000 cm^{-1} (500 nm) to the red and the red one starting from about 16700

cm^{-1} (600 nm). The former is assigned to the fluorescence from 1^1B_u , as is indicated by a good mirror-image relationship and a sufficient overlapping between the fluorescence and the $1^1A_g \rightarrow 1^1B_u$ absorption bands, while the latter is assigned to the fluorescence from 2^1A_g . The spectral shape of the 2^1A_g fluorescence of DP7 is quite similar to that of diphenyldodecahexaene ($n=6$) at room temperature.⁷ We could not determine the accurate fluorescence quantum yield of DP7 because of the weakness of the emission and appearance of the strong Raman and Rayleigh scattering from the solvent, but it was evaluated to be 10^{-5} – 10^{-4} . The excitation spectra obtained by monitoring the 2^1A_g and 1^1B_u fluorescence agrees with the absorption spectrum. Further, the observed emission spectral shapes do not show significant temperature dependence in a range from 10 to 40 °C. It is clearly seen in Fig. 2 that the relative intensity of the 2^1A_g fluorescence to the 1^1B_u fluorescence changes significantly depending on the solvent.

As is seen in Fig. 3 (and also in Fig. 5), DP7 exhibits anti-Kasha emission [the $1^1B_u(S_2)$ fluorescence] beside the 2^1A_g fluorescence in solution at room temperature. Diphenylhexatriene (DP3) and diphenyloctatetraene (DP4) also are known to emit the 2^1A_g and 1^1B_u fluorescence in solution at temperatures near room temperature.^{11–13} However, the mechanism for the occurrence of the 1^1B_u fluorescence of DP7 seems to be different from that reported for DP3 and DP4. With DP3 and DP4 the 1^1B_u fluorescence occurs as the results of the thermal population from the 2^1A_g state, i.e., the thermally activated delayed fluorescence.^{11–13} On the other hand, the 1^1B_u fluorescence of DP7 is considered to occur as the result of the inefficient internal conversion from 1^1B_u to 2^1A_g due to a large energy separation between the two excited states, i.e., the prompt fluorescence.

A. Franck–Condon analysis of the spectra

In order to determine the relative intensities for the fluorescence and absorption quantitatively, all the spectra data were fitted by sum of Gaussians, where the intensity $I(\nu)$ at wave number ν was assumed to have the form,

$$I(\nu) = I_0(\nu_0) \times \exp[-(\nu - \nu_0)^2 / \sigma^2], \quad (1)$$

where ν_0 is the wave number at the Gaussian center, $I_0(\nu_0)$

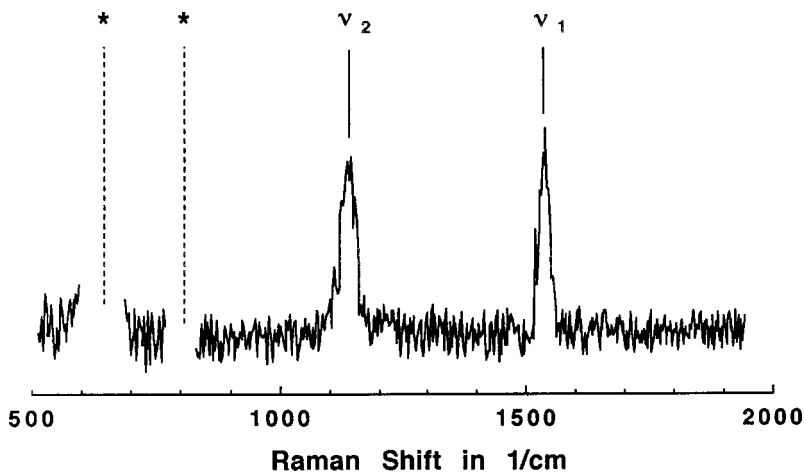


FIG. 4. Raman spectrum of DP7 in CS_2 at 35 °C. The locations of the Raman peaks from the solvent are indicated by asterisks.

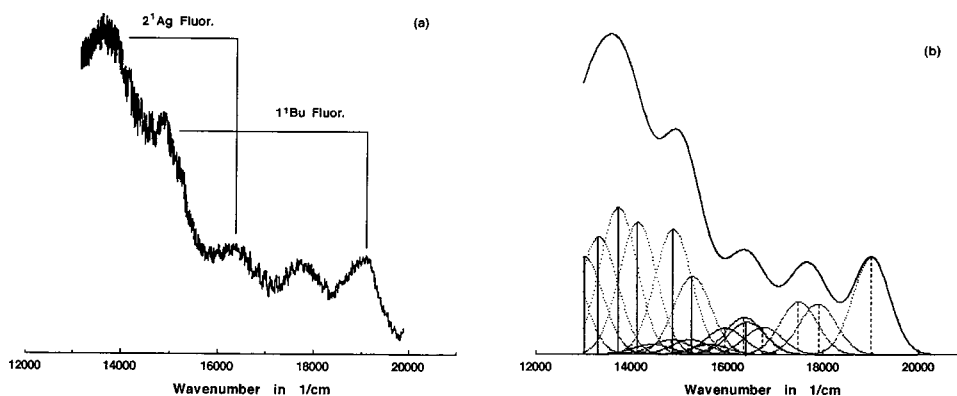


FIG. 5. Corrected emission spectrum of DP7 in CS_2 at 18°C (a) and the calculated spectrum (b). In (b) Gaussian amplitudes are indicated by broken-line sticks for the 1^1B_u fluorescence and by solid-line sticks for the 2^1A_g fluorescence. Gaussians width σ is kept constant for each of the 1^1B_u ($\sigma=700\text{ cm}^{-1}$) and 2^1A_g fluorescence ($\sigma=630\text{ cm}^{-1}$) irrespective of the mode.

is the amplitude and σ is the width. The spectra were fitted using Gaussians corresponding to the 0–0, 0–1, 0–2, and 0–3 for the $\text{C}=\text{C}(\nu_1)$ and $\text{C}-\text{C}(\nu_2)$ symmetric stretching modes as well as their combination modes by varying $I_0(\nu_0)$ and σ to get the Gaussian amplitudes, $I_0(\nu_0)$. The frequencies of the ν_1 and ν_2 modes in the ground state are obtained to be 1536 ± 2 and $1136\pm 2\text{ cm}^{-1}$ from the Raman spectrum displayed in Fig. 4. The width σ is kept constant irrespective of the modes. Examples of the calculated emission and absorption spectra are shown, respectively, in Figs. 5 and 6 for DP7 in CS_2 . These inhomogeneously broadened solution spectra can be reproduced reasonably by using only two intrinsic harmonic normal modes. In the case of absorption, when twelve Gaussians were fit to the first 5000 cm^{-1} of the spectrum, the measured and calculated spectra were almost indistinguishable to each other (see Fig. 6).

The intensity in a given vibronic band, $I_0(\nu_0)$, is assumed to be proportional to the Franck–Condon factor which is described by the harmonic oscillator wave function basis. Thus, we have

$$I_0(\nu_0) = \text{const.} \times \prod_i |\langle \phi_{i,m}(Q_{i,g}) | \phi_{i,n}(Q_{i,e}) \rangle|^2, \quad (2)$$

where i is the number of normal modes, and m and n are the vibrational quantum numbers. The overlap integrals, $\langle \phi_{i,m}(Q_{i,g}) | \phi_{i,n}(Q_{i,e}) \rangle$, which are a function of displacement of the excited electronic state (e) potential curve for each normal coordinate from the corresponding ground state

(g) as well as of the corresponding vibrational frequencies in the excited and ground states, can be simply calculated with the recurrence relations derived by Manneback.¹⁴

The Franck–Condon envelop of the 1^1B_u fluorescence is qualitatively different from that of the 2^1A_g fluorescence, resembling more closely the Franck–Condon envelop of the 1^1B_u absorption [see Fig. 3(b) and Table I]. Both of the ν_1 and ν_2 intensities decrease monotonously with increasing the vibrational quantum number n in the 0– n transition for the 1^1B_u fluorescence and 1^1B_u absorption, while the ν_1 and ν_2 intensities show maxima, respectively, at the 0–1 and 0–2 transitions for the 2^1A_g fluorescence. The displacements calculated using the data shown in Table I are summarized in Table II. The displacements of the ν_1 and ν_2 modes as obtained from the 1^1B_u fluorescence are smaller than those from the 2^1A_g fluorescence by a factor of near 1/2, but correspond quite closely to the displacements obtained by fitting the 1^1B_u absorption spectrum. This is what we expected when the 1^1B_u fluorescence and absorption spectra are in a mirror-image relationship.

B. Solvent-polarizability dependence of the fluorescence spectrum

As are shown in Figs. 3 and 5 the relative intensity of the 2^1A_g and 1^1B_u fluorescence of DP7 changes markedly depending on the solvent. In order to analyze the relative 2^1A_g

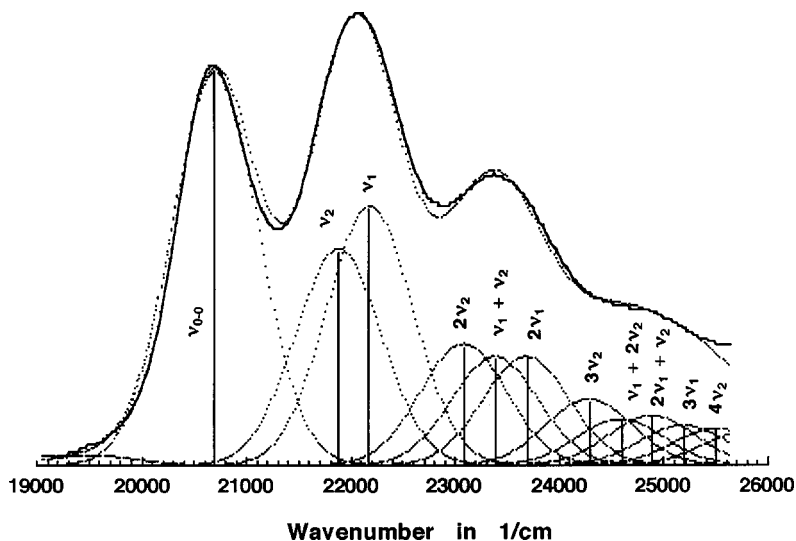


FIG. 6. Absorption spectrum of DP7 in CS_2 at 18°C (solid line spectrum) and the calculated spectrum with fitted Gaussians (dotted line curves). Gaussian amplitudes are indicated by solid-line sticks along with the assignments. The width σ is kept constant for all the Gaussians used, irrespective of the mode ($\sigma=580\text{ cm}^{-1}$).

TABLE I. Amplitudes and wave numbers of the ν_1 and ν_2 modes for the Franck–Condon analyses obtained from the Gaussian fittings of the 2^1A_g and 1^1B_u fluorescence and the 1^1B_u absorption spectra of DP7 in CS_2 at 18 °C.

Assignment	$\pm\Delta\nu$ (cm ⁻¹) from the origin ^a		Amplitudes ^b		
	$1^1A_g \leftarrow 2^1A_g$	$1^1A_g \rightarrow 1^1B_u$	$1^1A_g \leftarrow 2^1A_g$	$1^1A_g \leftarrow 1^1B_u$	$1^1A_g \rightarrow 1^1B_u$
ν_{0-0}	0	0	1.00	1.00	1.00
ν_2	-1136	+1200	2.42	0.52	0.55
ν_1	-1536	+1500	3.88	0.54	0.66
$2 \times \nu_2$	-2272	+2400	4.09	0.28	0.31
$\nu_1 + \nu_2$	-2672	+2700	4.55	0.38	0.28
$2 \times \nu_1$	-3072	+3000	3.63	0.27	0.28
$3 \times \nu_2$	-3408	+3600	3.03	0.10	0.17
$\nu_1 + 2 \times \nu_2$	-3808	+3900	3.33	0.15	0.12
$2 \times \nu_1 + \nu_2$	-4208	+4200	...	0.15	0.13
$4 \times \nu_2$	-4544	+4800	...	0.10	0.08
$3 \times \nu_1$	-4608	+4500	0.09

^aError of ± 2 cm⁻¹ for the $1^1A_g \leftarrow 2^1A_g$ and ± 20 cm⁻¹ for the $1^1A_g \leftarrow 1^1B_u$ transition.

^bError, ± 0.02 .

and 1^1B_u fluorescence intensities systematically, the emission spectra of DP7 were measured in mixtures of carbon tetrachloride and diiodomethane mixed in different ratios. Further, to treat the observed spectral intensity ratios quantitatively, only the second band of the 2^1A_g and the first band of the 1^1B_u fluorescence spectra were reproduced using the fitted Gaussian amplitudes, and the intensities of the reproduced bands are treated as the 2^1A_g and 1^1B_u fluorescence intensities. Dependence of the solvent polarizability on the $2^1A_g \leftarrow 1^1B_u$ energy separation of diphenylpolyenes has been well rationalized.² In Fig. 7 relation between the $2^1A_g/1^1B_u$ fluorescence-intensity ratio, I_1/I_2 , thus obtained and the $2^1A_g \leftarrow 1^1B_u$ energy separation, ΔE , is presented. It is seen that in carbon tetrachloride–diiodomethane mixtures, the ratio I_1/I_2 decreases monotonously with increasing ΔE .

Since the observed 1^1B_u fluorescence of DP7 is considered to be prompt fluorescence which occurs as the result of the inefficient internal conversion from 1^1B_u to 2^1A_g , the ratio of the 2^1A_g -fluorescence to the 1^1B_u -fluorescence quantum yield is given by

$$\Phi(1^1A_g)/\Phi(1^1B_u) = k_1/k_2 \times \phi(2 \rightarrow 1) \times (k_2 + k_{2n})/(k_1 + k_{1n}), \quad (3)$$

where k_1 and k_2 are the radiative rate constants, k_{1n} and k_{2n} are nonradiative rate constants of the 2^1A_g and 1^1B_u states, respectively, and $\phi(2 \rightarrow 1)$ is the internal conversion efficiency from 1^1B_u to 2^1A_g . Since the $\Phi(1^1A_g)$ and $\Phi(1^1B_u)$ values of DP7 are in the order of 10^{-4} – 10^{-5} , we can safely assume $k_{1n} \gg k_1$ and $k_{2n} \gg k_2$. Then, Eq. (3) is rewritten as

$$\Phi(1^1A_g)/\Phi(1^1B_u) \cong k_1/k_2 \times \phi(2 \rightarrow 1) k_{2n}/k_{1n}. \quad (4)$$

Although the 1^1B_u absorption spectrum exhibits a significant redshift with increasing the solvent polarizability, the locations of the apparent 2^1A_g origins in the fluorescence and absorption spectra are almost unchanged as are seen in Figs. 2, 3, and 5. Further, the $1^1B_u \rightarrow 2^1A_g$ internal conversion rates recently reported are almost constant for diphenylpolyenes with n from 3 to 7.¹⁵ Hence, it is not unreason-

able to assume that the k_{1n} , k_{2n} , and $\phi(2 \rightarrow 1)$ values do not depend strongly on ΔE which changes only from 3500 to 5000 cm⁻¹ by varying the solvent polarizability. Hence, we have

$$\Phi(1^1A_g)/\Phi(1^1B_u) \cong \text{const.} \times k_1/k_2. \quad (5)$$

The ratio k_1/k_2 in Eq. (5) can be regarded as a value equivalent to the ratio of the oscillator strength for the $1^1B_u \leftarrow 1^1A_g$, f_2 , to that for the $2^1A_g \leftarrow 1^1A_g$ transition, f_1 , through the relation $k_1/k_2 = f_1/f_2$. If we further assume that all of the radiative strength for the 2^1A_g fluorescence originates from the coupling between 2^1A_g and 1^1B_u , the oscillator strength, f_1 , should obey an expression of the form,¹

$$f_1 = f_2 \langle \Psi(1^1A_g) | \mathcal{H}_{\text{int}} | \Psi(1^1B_u) \rangle^2 / \Delta E^2, \quad (6)$$

where the two excited states are mixed through an interaction operator, \mathcal{H}_{int} , which may be of vibronic in nature. It has been demonstrated that the coupling constant, $\langle \Psi(1^1A_g) | \mathcal{H}_{\text{int}} | \Psi(1^1B_u) \rangle$, is not a function of the solvent.¹⁶ Since the quantum-yield ratio is regarded as a value equivalent to the intensity ratio, I_1/I_2 , we finally have

$$I_1/I_2 \cong \text{const.} (1/\Delta E^2). \quad (7)$$

The data shown in Fig. 7 were analyzed on the basis of Eq. (7). As one can see in Fig. 7, the obtained data do not agree exactly with Eq. (7). However, considering the error in obtaining the intensity ratios and the approximations used for

TABLE II. Mode displacements in units of (amu)^{1/2} Å from Franck–Condon fits to the fluorescence and absorption spectra of DP7 in CS_2 at 18 °C. Frequencies used for the ν_1 (C=C) and ν_2 (C–C) modes are, respectively, 1536 and 1136 cm⁻¹ for 1^1A_g , 1740 and 1230 cm⁻¹ for 2^1A_g , and 1500 and 1200 cm⁻¹ for 1^1B_u . Mode frequencies in the 2^1A_g state of DP7 are estimated by the extrapolation of the data for diphenylhexatriene (Ref. 18) and diphenyldecapentaene (Ref. 6).

Mode	$2^1A_g \rightarrow 1^1A_g$ Fluor.	$1^1B_u \rightarrow 1^1A_g$ Fluor.	$1^1A_g \rightarrow 1^1B_u$ Abs.
ν_1	0.33 ± 0.02	0.18 ± 0.01	0.19 ± 0.01
ν_2	0.35 ± 0.03	0.19 ± 0.02	0.20 ± 0.03

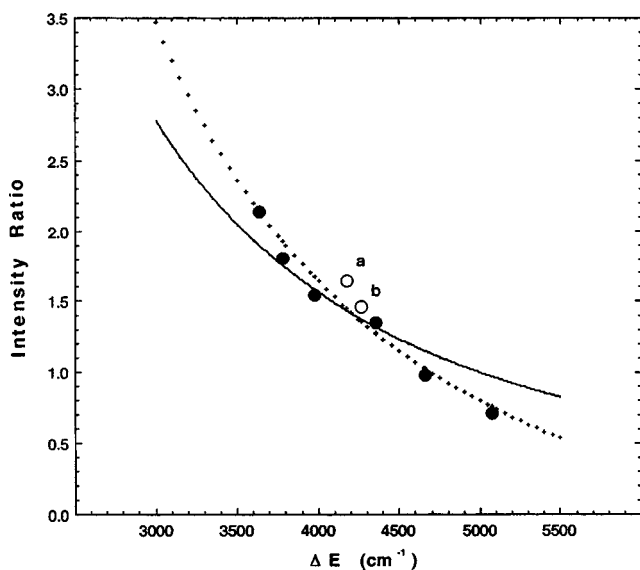


FIG. 7. $2^1A_g/1^1B_u$ fluorescence intensity-ratio, I_1/I_2 , plotted as a function of the $2^1A_g-1^1B_u$ energy separation, ΔE , for DP7 in solvents with different polarizabilities. The closed-circle plots are obtained in diiodomethane-carbon tetrachloride mixtures and the open-circle plots indicated by "a" and "b" are obtained in CS_2 and 1-bromonaphthalene, respectively. A solid-line curve is the one fitted to $I_1/I_2 = \text{const.}/\Delta E^2$, while a dotted-line curve is the one fitted to the data obtained in diiodomethane-carbon tetrachloride mixtures (see text). The location of the 2^1A_g state is tentatively taken at $16\,667\text{ cm}^{-1}$ (600 nm), while the first 1^1B_u absorption band is taken as the 1^1B_u origin for the evaluation of ΔE .

the derivation of Eq. (7), we can say that the plots shown in Fig. 7 are on a curve (a dotted-line curve) very close to the one obtained from Eq. (7) (a solid-line curve). Actually, the obtained plots fit well to the relation, $I_1/I_2 = c_1 \times (1/\Delta E^2) - c_2$ ($c_1, c_2 > 0$), rather than to Eq. (7). The small discrepancy may be arising in part from the error in evaluation of ΔE and the assumptions that k_{1n} , k_{2n} , and $\phi(2 \rightarrow 1)$ are treated as being invariant with ΔE as well as from the error introduced in obtaining the intensity ratios.

IV. CONCLUSIONS

The present results indicate that the $2^1A_g/1^1B_u$ fluorescence intensity-ratio of DP7 in solution is determined mainly by the coupling strength between 2^1A_g and 1^1B_u , i.e., the oscillator strength of the 2^1A_g state, which is dominated

by the $2^1A_g-1^1B_u$ energy separation. Fitting of the spectra with Gaussians reveals a large difference in the Franck-Condon envelopes between the 2^1A_g and 1^1B_u fluorescence spectra which is originating from the large difference in the C=C and C-C stretching mode displacements between the two excited states. This excited-state character seems to be common to all the fluorescent polyenes.¹⁷

Finally, it should be mentioned again that the assignment of the observed emission to the dual fluorescence of DP7 is guaranteed by a number of reasons: (a) The corrected excitation spectrum of the observed emission agrees with the absorption spectrum of DP7; (b) the spectral shape of the observed 2^1A_g fluorescence is quite similar to that of diphenyldodecahexaene ($n=6$) which is a closely relative of DP7;⁷ (c) the 1^1B_u fluorescence emission exhibits an expected mirror image relationship with the 1^1B_u absorption spectrum; (d) the measured 2^1A_g and 1^1B_u fluorescence spectra are reproduced reasonably by taking into account only the intrinsic C-C and C=C stretching modes of DP7; and (e) the 2^1A_g fluorescence spectrum starts to the red just at the wavelengths where the very weak absorption band is observed.

- ¹B. S. Hudson and B. E. Kohler, *J. Chem. Phys.* **59**, 4984 (1973).
- ²B. S. Hudson, B. E. Kohler, and K. Shulten, *Excited States* **5**, 1 (1982).
- ³B. E. Kohler, *Chem. Rev.* **93**, 41 (1993).
- ⁴T. Itoh and B. E. Kohler, *J. Phys. Chem.* **92**, 1807 (1988).
- ⁵M. T. Allen and D. G. Whitten, *Chem. Rev.* **89**, 1691 (1989).
- ⁶J. S. Horwitz, T. Itoh, B. E. Kohler, and C. W. Spangler, *J. Chem. Phys.* **87**, 2433 (1987).
- ⁷T. Itoh, B. E. Kohler, and C. W. Spangler, *Spectrochim. Acta, Part A* **50A**, 2261 (1994).
- ⁸S. M. Bachilo, C. W. Spangler, and T. Gillbro, *Chem. Phys. Lett.* **283**, 235 (1998).
- ⁹C. W. Spangler, R. K. McCoy, A. A. Dembek, L. S. Sapochak, and B. D. Gates, *J. Chem. Soc., Perkin Trans. 1* **1**, 151 (1989).
- ¹⁰E. Lippert, W. Nagele, I. S-Blankenstein, U. Staiger, and W. Voss, *Z. Anal. Chem.* **170**, 1 (1959).
- ¹¹T. Itoh and B. E. Kohler, *J. Phys. Chem.* **91**, 1760 (1987).
- ¹²T. Itoh, *Chem. Phys. Lett.* **159**, 263 (1989).
- ¹³T. Itoh, *Bull. Chem. Soc. Jpn.* **75**, 1973 (2002).
- ¹⁴C. Manneback, *Physica (Amsterdam)* **17**, 1001 (1951).
- ¹⁵Y. Hirata, K. Mashima, H. Fukumoto, K. Tani, and T. Okada, *Chem. Phys. Lett.* **308**, 167 (1999).
- ¹⁶J. R. Andrews and B. S. Hudson, *J. Chem. Phys.* **68**, 4587 (1978).
- ¹⁷B. E. Kohler and T. Itoh, *J. Phys. Chem.* **92**, 5120 (1988).
- ¹⁸B. E. Kohler and T. A. Spiglanin, *J. Chem. Phys.* **80**, 5465 (1984).